

The First Bowl-Shaped Stable Neutral Radical with a Corannulene System: Synthesis and Characterization of the Electronic Structure

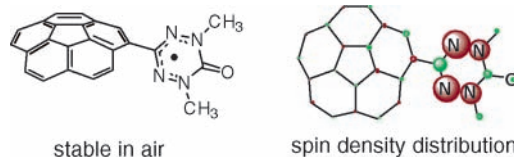
Yasushi Morita,^{*,†,‡} Shinsuke Nishida,[†] Tadahiro Kobayashi,[†] Kozo Fukui,[‡] Kazunobu Sato,[§] Daisuke Shiomu,[§] Takeji Takui,^{*,§} and Kazuhiro Nakasuji^{*,†}

Department of Chemistry, Graduate School of Science, Osaka University, Toyonaka, Osaka 560-0043, Japan, Departments of Chemistry and Materials Science, Graduate School of Science, Osaka City University, Sumiyoshi-ku, Osaka 558-8585, Japan, and PRESTO-JST, Hon-cho, Kawaguchi, Saitama 332-0012, Japan

morita@chem.sci.osaka-u.ac.jp

Received February 7, 2004

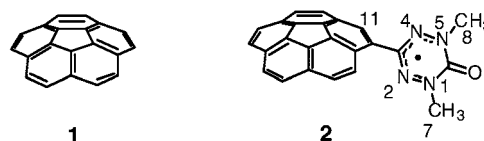
ABSTRACT



A bowl-shaped neutral radical with a corannulene system has been designed and synthesized for the first time as a stable solid in air. An unequivocal characterization of the electronic properties of the radical shows that an appreciable amount of spin delocalization extends onto the corannulene unit's curved surface.

The stabilization and isolation of novel organic neutral radicals are not only important subjects in the mechanistic understanding of many organic transformations¹ but also the focus of the current topics in the synthetic organic chemistry underlying molecule-based magnetic materials.² It is widely accepted that a sterically congested organic radical in which the odd electrons are delocalized over a conjugated π -electron network is significantly more stable than a corresponding less sterically hindered nondelocalized radical (steric and resonance stabilization effects).³ Recently, we have succeeded in the synthesis of new stable organic neutral radicals based on the phenalenyl skeleton by introduction of *tert*-

butyl groups and heteroatomic substitutions into planar π -electronic systems.⁴



In contrast, neutral radicals with bowl-shaped (curved surface) π -electronic structures as seen in fullerene derivatives have only been generated as unstable molecules in solution states.⁵ Still, corannulene (**1**) chemistry has become a focus of studies on metal complexes of curved surface π -electrons.⁶ Thus, we decided to study whether the stabilization effects established for planar π -radical systems also

[†] Osaka University.

[‡] PRESTO-JST.

[§] Osaka City University.

(1) Fossey, J.; Lefort, D.; Sorba, J. *Free Radicals in Organic Chemistry*; John Wiley & Sons: Chichester, 1995; pp 1–307.

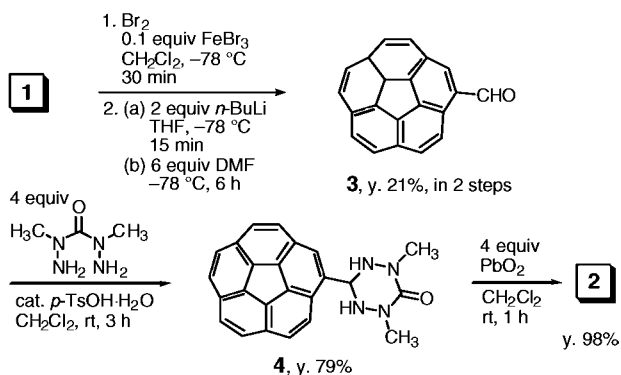
(2) (a) Itoh, K.; Kinoshita, M., Eds. *Molecular Magnetism*; Kodansha, and Gordon and Breach Science Publishers: Tokyo, 2000; pp 1–347. (b) Lahti, P. M., Ed. *Magnetic Properties of Organic Materials*; Marcel Dekker: New York, 1999; pp 1–728.

(3) (a) Smith, M. B.; March, J. *March's Advanced Organic Chemistry Reaction, Mechanisms, and Structure*, 5th ed.; John Wiley & Sons: New York, 2001; pp 238–245. (b) Rüchardt, C. *Top. Curr. Chem.* **1980**, *88*, 1–32.

apply to curved surface π -radical systems. We emphasize that the occurrence of dynamic spin polarization in high spin states of curved surface π -systems such as fullerenes is a crucial model for the estimation of three-dimensional inter-electronic exchange and dipolar interactions.⁷ As the first step for the evaluation of such π -spin effects, we have designed a new neutral oxoverdazyl radical conjugated with corannulene system **2**.⁸ In this report, we describe the synthesis of this bowl-shaped stable neutral radical and its electronic properties as probed by ESR/ENDOR spectra, DFT calculations, UV-vis, and CV spectra.

Radical **2** was synthesized from corannulene **1** in four steps (Scheme 1). The monobromo derivative of **1**, prepared

Scheme 1. Preparation of **2** from Corannulene **1**



by a literature procedure,¹⁰ was converted to aldehyde **3** by treatment with 2 equiv of *n*-BuLi followed by DMF.¹¹ The

(4) (a) Morita, Y.; Ohba, T.; Haneda, N.; Maki, S.; Kawai, J.; Hatanaka, K.; Sato, K.; Shiomi, D.; Takui, T.; Nakasujii, K. *J. Am. Chem. Soc.* **2000**, *122*, 4825–4826. (b) Morita, Y.; Maki, S.; Fukui, K.; Ohba, T.; Kawai, J.; Sato, K.; Shiomi, D.; Takui, T.; Nakasujii, K. *Org. Lett.* **2001**, *3*, 3099–3102. (c) Morita, Y.; Nishida, S.; Kawai, J.; Fukui, K.; Nakazawa, S.; Sato, K.; Shiomi, D.; Takui, T.; Nakasujii, K. *Org. Lett.* **2002**, *4*, 1985–1988. (d) Morita, Y.; Aoki, T.; Fukui, K.; Nakazawa, S.; Tamaki, K.; Suzuki, S.; Fuyuhiko, A.; Yamamoto, K.; Sato, K.; Shiomi, D.; Naito, A.; Takui, T.; Nakasujii, K. *Angew. Chem., Int. Ed.* **2002**, *41*, 1793–1796. (e) Morita, Y.; Kawai, J.; Fukui, K.; Nakazawa, S.; Sato, K.; Shiomi, D.; Takui, T.; Nakasujii, K. *Org. Lett.* **2003**, *5*, 3289–3291.

(5) Krusic, P. J.; Wasserman, E.; Keizer, P. N.; Morton, J. R.; Preston, K. F. *Science* **1991**, *254*, 1183–1185. See also overview of open-shell species based on fullerene derivatives: Tumanskii, B., Kalina O., Eds. *Radical Reactions of Fullerenes and their Derivatives*; Kluwer Academic Publishers: Dordrecht, 2001, pp 1–192.

(6) Petrukhina, M. A.; Andreini, K. W.; Mack, J.; Scott, L. T. *Angew. Chem., Int. Ed.* **2003**, *42*, 3375–3379 and references therein.

(7) (a) Surján, P. R.; Németh, K.; Bennati, M.; Grupp, A.; Mehring, M. *Chem. Phys. Lett.* **1996**, *251*, 115–118. (b) Shohoji, M. C. B. L.; Franco, M. L. T. M. B.; Lazana, M. C. R. L. R.; Nakazawa, S.; Sato, K.; Shiomi, D.; Takui, T. *J. Am. Chem. Soc.* **2000**, *122*, 2962–2963. (c) Visser, J.; Groenen, E. J. *J. Chem. Phys. Lett.* **2002**, *356*, 43–48.

(8) As open-shell species derived from corannulene system, a radical anion was generated by reduction of **1** in a solution in a sealed tube and characterized by ESR measurements. However, this species is known to be difficult to handle in air; see for example: (a) Janata, J.; Gendell, J.; Ling, C.-Y.; Barth, W.; Backes, L.; Mark, Jr., H. B.; Lawton, R. G. *J. Am. Chem. Soc.* **1967**, *89*, 3056–3058. (b) Sato, T.; Yamamoto, A.; Tanaka, H.; *Chem. Phys. Lett.* **2000**, *326*, 573–579.

(9) We prepared **1** according to the following references with some modifications: (a) Seiders, T. J.; Elliott, E. L.; Grube, G. H.; Siegel, J. S. *J. Am. Chem. Soc.* **1999**, *121*, 7804–7813. (b) Sygula, A.; Rabideau, P. W. *J. Am. Chem. Soc.* **2000**, *122*, 6323–6324. (c) Xu, G.; Sygula, A.; Marcinow, Z.; Rabideau, P. W. *Tetrahedron Lett.* **2000**, *41*, 9931–9934.

radical precursor **4** was prepared by condensation of **3** with 2,4-dimethylcarbonohydrazide in the presence of a catalytic amount of *p*-TsOH·H₂O in CH₂Cl₂ at room temperature.¹² The neutral radical **2**¹³ was quantitatively obtained as a vivid red powder by treatment of **4** with active PbO₂ in CH₂Cl₂. In the solid state, most of the radical **2** remains unchanged in air for a few weeks. The radical is also stable for a long period of time in degassed toluene but decomposes in the presence of atmospheric oxygen.

Radical **2** in degassed toluene solution (1.0×10^{-4} M) shows well-resolved hyperfine coupling in the ESR spectrum observed at 293 K. The spectrum was obtained at 12.5 kHz field modulation in order to avoid line shape distortion due to sideband formation (Figure 1a) with such narrow line

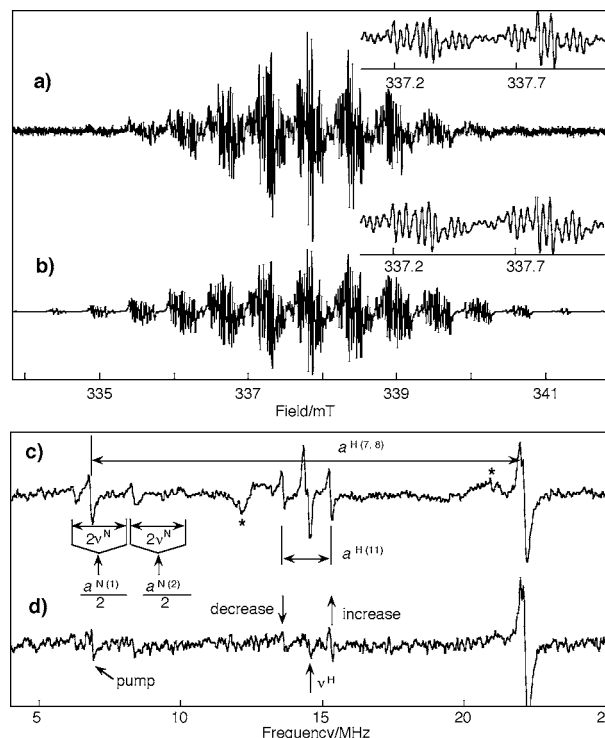


Figure 1. (a) Observed hyperfine ESR spectrum at 293 K (microwave frequency 9.477225 GHz) and (b) the corresponding simulated spectrum, (c) ENDOR, and (d) TRIPLE (pump frequency, 6.81 MHz) spectra at 270 K for **2** in toluene (1.0×10^{-4} M). The asterisks indicate spectrometer artifacts.

width (0.016 mT). ENDOR spectroscopy (Figure 1c) shows two pairs of lines that are attributed to the two kinds of nitrogens, with splittings due to methyl protons on oxoverdazyl and methyne proton on the corannulene skeleton.¹⁴ Importantly, the sharp line at about 14.5 MHz is attributable

(10) Seiders, T. J.; Elliott, E. L.; Grube, G. H.; Siegel, J. S. *J. Am. Chem. Soc.* **1999**, *121*, 7804–7813.

(11) (a) Scott, L. T.; Hashemi, M. M.; Bratcher, M. S. *J. Am. Chem. Soc.* **1992**, *114*, 1920–1921. (b) Scott, L. T.; Bronstein, H. E.; Preda, D. V.; Ansems, R. B. M.; Bratcher, M. S.; Hagen, S. *Pure Appl. Chem.* **1999**, *71*, 209–219. Full assignment of ¹H NMR spectrum in terms of NOESY, COSY, HMQC, and HMBC measurements and elemental analysis of **3**; see Supporting Information.

to other protons on the corannulene skeleton. The relative signs of the hyperfine coupling constants (hfccs) of two types of protons were determined by TRIPLE spectroscopy (Figure 1d) to be the same. The spectral simulation (Figure 1b) was satisfactory on the basis of the set of hfccs obtained by ENDOR spectroscopy. The g -value of **2** was determined to be 2.0041, which is the same as that of 3-(4-methoxyphenyl)-oxoverdazyl derivative **5**.¹⁵ The protons and nitrogens of **2** were assigned in terms of the spin density distribution calculated by the DFT method using the optimized structure (Figure 2).^{16,17} Both experiment and theory show that an

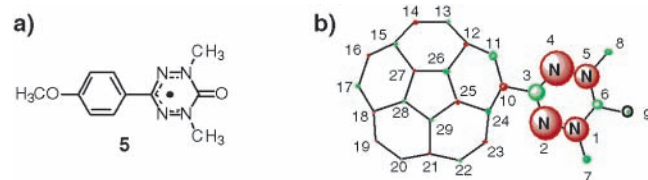


Figure 2. (a) Molecular structure of **5** and (b) spin density distribution of **2** calculated by the DFT method.¹⁶ Green-colored and red-colored circles denote negative and positive spin densities, respectively.

appreciable amount of spin density is delocalized onto the corannulene moiety with most of the spin density localized on the oxoverdazyl moiety (Table 1).

Table 1. Observed and Calculated Hfccc for **2**^a

	a (mT)			
	N(1, 5)	N(2, 4)	H(7, 8)	H(11)
obsd, ENDOR ^b	± 0.519	± 0.658	$+0.546$	$+0.060$
obsd, ESR ^c	± 0.519	± 0.650	$+0.546$	$+0.061$
calcd ^d	$+0.389$	$+0.542$	$+0.584$	$+0.063$

^a Relative signs of the hfccs were determined by TRIPLE spectroscopy. ^b Hfccc were determined by ENDOR spectrum in a toluene solution at 270 K. ^c Hfccc were determined by ESR spectrum in a toluene solution at 290 K and spectral simulation. ^d Values were calculated by using Gaussian 98 with the UBLYP/6-31G**//UBLYP/6-31G** method.

To obtain further information on the electronic structure of this radical, we have measured UV–vis spectra and cyclic voltammetry for **1**,^{9a,18} **2**, **4**, and **5** in CH₃CN. The solution UV spectra are shown in Figure 3.¹⁹ The absorption of the

(12) Selected physical data: **4**, mp 197–198 °C.; ¹H NMR (600 MHz, CDCl₃) δ 3.29 (s, 6), 4.73 (d, $J = 10.7$ Hz, 2), 5.58 (dt, $J = 10.5$ and 1.4 Hz, 1), 7.78 (d, $J = 8.8$ Hz, 1), 7.80 (d, $J = 8.8$ Hz, 1), 7.81 (d, $J = 8.8$ Hz, 1), 7.82 (d, $J = 8.2$ Hz, 1), 7.82 (d, $J = 8.2$ Hz, 1), 7.83 (d, $J = 8.5$ Hz, 1), 7.85 (d, $J = 8.8$ Hz, 1), 7.90 (d, $J = 1.4$ Hz, 1), 8.20 ppm (d, $J = 8.8$ Hz, 1); IR (KBr) 3227, 3024, 2925, 1623 cm⁻¹; EI-MS, m/z 378 (M⁺, 15%); HRMS-EI, m/z calcd for C₂₄H₁₈N₄O (M⁺), 378.1482; found, 378.1475. Anal. Calcd for C₂₄H₁₈N₄O: C, 76.17; H, 4.79; N, 14.81. Found: C, 75.72; H, 4.82; N, 14.49. See also Supporting Information.

(13) Selected physical data: **2**, mp 159–160 °C (dec); TLC R_f 0.73 (THF); IR (KBr) 3031, 2931, 1685 cm⁻¹; EI-MS, m/z 375 (M⁺, 31%); HRMS-EI m/z calcd for C₂₄H₁₅N₄O (M⁺) 375.1248, found 375.1235. Anal. Calcd for (C₂₄H₁₅N₄O)(CH₂Cl₂)_{0.45}: C, 71.00; H, 3.87; N, 13.55. Found: C, 71.00; H, 3.90; N, 13.56.

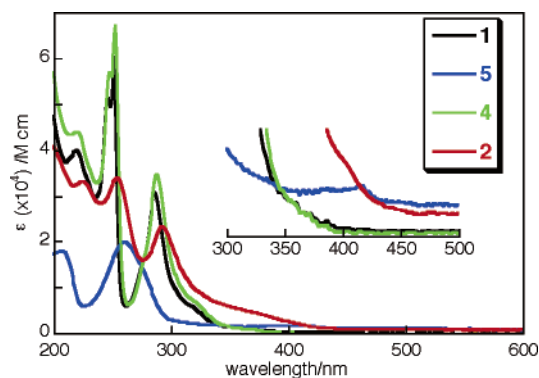


Figure 3. UV–vis spectra of **1** (1.1×10^{-5} M, black line), **2** (1.4×10^{-5} M, red line), **4** (1.0×10^{-5} M, green line), and **5** (1.1×10^{-5} M, blue line) in CH₃CN solutions. Spectra for **1**, **4**, and **5** were measured using an open quartz cell, while spectra for **2** were measured using a sealed quartz cell. The ordinate scale of the inset is magnified 40 times.¹⁹

oxoverdazyl moiety of **2** was observed as a broad band between 300 and 450 nm, overlapping with those of the corannulene moiety. Since the peak maxima for **2** shift by only 3–6 nm relative to the corresponding peaks for **1** in the region of 220–300 nm, we suggest that the π -conjugation between the corannulene moiety and the oxoverdazyl unit of **2** is weak in the ground state.

The cyclic voltammograms for **1**,^{8a,9a} **2**, **4**, and **5**²⁰ in CH₃CN solution are shown in Figure 4. The reduction potentials for the corannulene moieties for **2** and **4** are nearly identical to that for corannulene **1**. The radical **2**, however, shows an irreversible oxidation wave at +0.24 V (peak potential), while **5** shows a reversible oxidation wave at +0.24 V (half wave potential). These results indicate measurable electronic perturbation on the oxoverdazyl unit induced by the corannulene curved surface π -system.

(14) Since the condition $|a^N/2| > \nu^N$ (ν^N = nuclear Larmor frequency of ¹⁴N) is applied for the present case, a pair of ¹⁴N-ENDOR lines appear at $a^N/2 \pm \nu^N$ for each ¹⁴N hyperfine coupling. This explains the accidental overlapping of the two ENDOR lines, which resulted in an apparent single line at 8.25 MHz. ¹⁴N-TRIPLE measurements did not allow us to determine the relative signs of a^N .

(15) Neugebauer, F. A.; Fischer, H.; Siegel, R. *Chem. Ber.* **1988**, *121*, 815–822. As the microwave power was increased, the solution-ESR absorption of **2** was readily saturated as compared to that of **5**, reflecting a slow spin-relaxation behavior that may be caused by a slow molecular tumbling due to the sizable corannulene moiety. See Supporting Information.

(16) Spin densities for **2** were calculated by Gaussian 98 with the UBLYP/6-31G**//UBLYP/6-31G** method; see Supporting Information.

(17) (a) DFT calculation estimated that 6.3 and 93.7% of absolute spin densities are populated by the corannulene and oxoverdazyl moieties, respectively. (b) The oxoverdazyl moiety exhibits a torsion angle of 18.9° relative to the aromatic ring system of corannulene; see Supporting Information.

(18) (a) Barth, W. E.; Lawton, R. G. *J. Am. Chem. Soc.* **1966**, *88*, 380–381. (b) Grube, G. H.; Elliott, E. L.; Steffens, R. J.; Jones, C. S.; Baldrige, K. K.; Siegel, J. S. *Org. Lett.* **2003**, *5*, 713–716.

(19) There are few UV–vis spectra reported for corannulene derivatives: full absorption data are given in Supporting Information. See also: Verdieck, J. F.; Jankowski, W. A. In *Molecular Luminescence: An International Conference*; Lim, E. C., Ed.; W. A. Benjamin Inc.: New York, 1969; pp 829–836.

(20) For redox properties of the 1,5-dimethyl-6-oxoverdazyl system, see: Barr, C. L.; Chase, P. A.; Hicks, R. G.; Lemaire, M. T.; Stevens, C. L. *J. Org. Chem.* **1999**, *64*, 8893–8897.

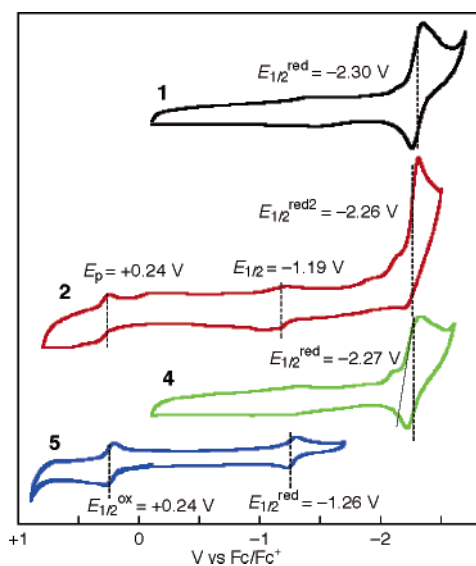


Figure 4. Cyclic voltammograms for **1**, **2**, **4**, and **5** at room temperature in CH₃CN solutions (3×10^{-3} M) containing Bu₄NClO₄ (0.1 M). For detailed experimental conditions, see Supporting Information.

In conclusion, we have for the first time accomplished the synthesis of a stable neutral radical **2** conjugated with a bowl-shaped π -electronic structure, in which the π -spin

density delocalization is extended on the corannulene moiety from the oxoverdazyl moiety.²¹ The high stability of this radical enables us to study dynamic behavior of the π -spin on the corannulene moiety that presumably is undergoing a concave–convex inversion in solution and to examine the solid-state properties related to intermolecular π -spin interactions of **2**. Furthermore, generation of a photoexcited triplet state of the corannulene moiety of **2** and elucidation of the intramolecular spin alignment with oxoverdazyl moiety also will be of great interest and will be reported in due course.^{22,23}

Acknowledgment. This work was supported by PRESTO-JST and The Sumitomo Foundation.

Supporting Information Available: Experimental procedure and full characterization data for new compounds, **2** and **4**, and the optimized structure of **2** by DFT calculation. This material is available free of charge via the Internet at <http://pubs.acs.org>.

OL0497786

(21) Preparation of imino nitroxide derivative of **1** was also carried out, and the result will be reported elsewhere.

(22) Intramolecular spin alignment between a stable radical and the metastable excited triplet state has been observed; see: Teki, Y.; Miyamoto, S.; Nakatsuji, M.; Miura, Y. *J. Am. Chem. Soc.* **2001**, *123*, 294–305 and references therein.

(23) For studies on fluorescence and phosphorescence of corannulene, see: (a) Bramwell, F. B.; Gendell, J. *J. Chem. Phys.* **1970**, *52*, 5656–5661. (b) Refs 9a, 18b, and 19.